



Microalgae as Soft Permeable Particles

Paula Araujo Gomes, Jean-Baptiste D'espinoze de Lacaille, Bruno Lartiges, Martin Maliet, Valérie Molinier, Nicolas Passade-Boupat, Nicolas Sanson

► To cite this version:

Paula Araujo Gomes, Jean-Baptiste D'espinoze de Lacaille, Bruno Lartiges, Martin Maliet, Valérie Molinier, et al.. Microalgae as Soft Permeable Particles. *Langmuir*, 2022, 38 (46), pp.14044-14052. 10.1021/acs.langmuir.2c01735 . hal-03951153

HAL Id: hal-03951153

<https://hal.science/hal-03951153>

Submitted on 22 Jan 2023

HAL is a multi-disciplinary open access archive for the deposit and dissemination of scientific research documents, whether they are published or not. The documents may come from teaching and research institutions in France or abroad, or from public or private research centers.

L'archive ouverte pluridisciplinaire **HAL**, est destinée au dépôt et à la diffusion de documents scientifiques de niveau recherche, publiés ou non, émanant des établissements d'enseignement et de recherche français ou étrangers, des laboratoires publics ou privés.

Microalgae as soft permeable particles

Paula Araujo Gomes,^{†,‡,¶} Jean-Baptiste d'Espinose de Lacaillerie,^{*,†,‡} Bruno Lartiges,[§] Martin Maliet,[†] Valérie Molinier,^{¶,||} Nicolas Passade-Boupat,^{¶,||} and Nicolas Sanson^{*,†,‡}

[†]*Soft Matter Sciences and Engineering Laboratory, ESPCI Paris, Université PSL, Sorbonne Université, CNRS UMR 7615, 10 Rue Vauquelin, F-75005 Paris, France*

[‡]*Laboratoire Physico-Chimie des Interfaces Complexes, ESPCI Paris, 10 Rue Vauquelin, F-75231 Paris, France*

[¶]*TotalEnergies OneTech, Pôle d'Etudes et Recherche de Lacq, BP 47, 64170 Lacq, France*

[§]*Géosciences Environnement Toulouse (GET), Université de Toulouse 3 (Paul Sabatier), 14 Avenue Edouard Belin, 31400 Toulouse, France*

^{||}*Laboratoire Physico-Chimie des Interfaces Complexes, Bâtiment CHEMSTARTUP, Route Départementale 817, 64170 Lacq, France*

E-mail: jean-baptiste.despinose@espci.fr; nicolas.sanson@espci.fr

Abstract

The colloidal stability of non-motile algal cells in water drives their distribution in space. An accurate description of the interfacial properties of microalgae is therefore critical to understand how microalgae concentrations can change in their biotope or during harvesting processes. Here, we probe the surface charges of three unicellular algae - *Chlorella vulgaris*, *Nannochloropsis oculata*, and *Tetraselmis suecica* - through their electrophoretic mobility. Ohshima's soft particle theory describes the electrokinetic properties of particles covered by a permeable polyelectrolyte layer, a usual case

for biological particles. The results appear to fit the predictions of Ohshima’s theory, proving that all three microalgae behave electrokinetically as soft particles. This allowed us to estimate two characteristic parameters of the polyelectrolyte external layer of microalgae: the volume charge density and the hydrodynamic penetration length. Results were compared with transmission electron microscopy observations of the algal cells’ surfaces, and in particular of their extracellular polymeric layer which was identified with the permeable shell evidenced by electrophoretic measurements. Noticeably, the algal surface potentials estimated from electrophoretic mobility using the soft particle theory are less negative than the apparent zeta potentials. This finding indicates that electrostatics are expected to play a minor role in phenomena of environmental and industrial importance, such as microalgae aggregation or adhesion.

Introduction

In recent years, microalgae have garnered increasing attention because of their various biotechnological applications, particularly for biofuel production, water treatment, and greenhouse gas emission mitigation^{1,2}. Despite the promising uses of these microorganisms, the harvesting step’s high energy cost is currently a limiting factor in microalgae production³. Microalgae harvesting may include two steps: a pre-concentration of the algae culture followed by a dewatering process consisting of separating the cells from the aqueous medium⁴. To achieve this, several methods such as centrifugation, sedimentation, filtration, flotation, and coagulation/flocculation exist with their relative advantages and disadvantages⁵. For instance, centrifugation is a high-efficiency harvesting method, however, it is too expensive for large-scale applications⁶. In order to achieve cost-efficiency in large-scale production, a low-cost concentration method such as flocculation can be implemented before a less demanding physical separation⁷.

Microalgae are microscopic organisms possessing a layer of extracellular polymeric substances (EPS) at their surface which governs, among other things, the physicochemical prop-

erties of microalgae in aqueous media⁸ and consequently their dispersion state, their interfacial behavior, and their adhesion^{9,10}. Therefore, a better understanding of algae surface physics is particularly interesting to enhance cell-cell adhesion, thus favoring flocculation.

Conceptually, microalgae can be seen as micrometer sized particles having a non-permeable core surrounded by a charged polyelectrolyte layer in an electrolyte solution. Classically, the electrical properties of colloidal particles are modeled assuming they are non-permeable to electrolyte ions and flow, i.e., hard particles, and these properties are expressed in terms of zeta potential. However, as described above, bioparticles such as microalgae or bacterial cells possess permeable charged EPS layers on their surface¹¹. Therefore, accounting for their electrical properties through the values of zeta potential is not suitable.

Over the years, numerous studies investigated hard particles surrounded by a permeable polyelectrolyte layer, called soft particles^{12–15}. A schematic representation of a soft charged particle can be seen in Figure 1. A significant contribution to describing the electrokinetic behavior of a soft particle was made by Ohshima^{11,12}, whose model is the most widely accepted. In short, the soft particle theory is based on the Poisson-Boltzmann equation for the electric potential distribution, the Navier-Stokes equation for the liquid flow, and, to account for the polyelectrolyte layer contribution, a Debye-Bueche model is used^{16,17}. General ex-

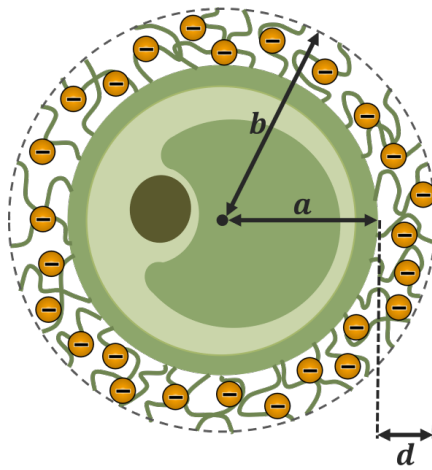


Figure 1: Schematic representation of a soft charged particle with total radius b composed of a hard core of radius a and a permeable charged polymeric layer of thickness d .

pressions can be written from the soft particle theory to predict electrophoretic mobility, but they can only be solved numerically. However, within given sets of approximations, analytic solutions can be derived and applied in many relevant cases^{12,18–20}.

This soft particle formalism has already been applied to many particles²¹ such as synthetic microgels^{22,23}, humic substances²⁴, natural latex particles^{25,26}, yeast^{27,28} and bacteria^{29,30}. To the best of our knowledge, there is no study reporting the application of the soft particle theory to microalgae yet. Therefore, the purpose of this study is to evaluate the applicability of soft particle theory to describe the electrostatic behavior of unicellular microalgae. To that effect, the electrokinetic behavior of different microalgae was assessed experimentally and compared to the predictions of the soft particle theory considering their cell’s surface structure. Three species were considered: one freshwater species, *Chlorella vulgaris* (*C. vulgaris*), and two seawater ones, *Nannochloropsis oculata* (*N. oculata*) and *Tetraselmis suecica* (*T. suecica*). Then, the charge density of the polyelectrolyte layer (ZN) and hydrodynamic softness (λ_{shell}) of each microalga was evaluated by fitting the data to the soft particle predictions. To validate the applicability of the surface properties obtained by considering the microalgae as soft colloids, the confidence interval of estimated parameters was calculated. Finally, the extracted parameters, charge density and penetration length, combined with transmission electron microscopy (TEM) observations provided detailed insights into the algae cells’ surfaces and consequently a better understanding of their behavior in suspension.

Materials and Methods

Microalgal Strains

C. vulgaris (CA104), *N. oculata* (CA101), and *T. suecica* (CA106) in the exponential growth phase were obtained from Greensea culture collection at Mèze, France. The cultures were stored in the dark at 4 °C in the refrigerator and used within 3 weeks of receipt.

Electrophoretic Mobility

For electrophoretic mobility measurements, the cells were centrifuged at 20 °C for 20 min under 3000×g, washed, and resuspended in KNO₃ solutions with adjusted ionic strengths in the range of 1–200 mM with a final cell concentration of approximately 10⁷ cells/mL. The cell concentration was estimated using a Neubauer counting chamber (Blaubrand, Germany) with a depth of 0.1 mm. Cell integrity was evaluated before and after centrifugation with an optical inverted microscope in transmitted light (Zeiss Axio Observer A1).

The electrophoretic mobility was measured as a function of the ionic strength of the suspensions using a Zetasizer Nano ZS (Malvern, UK) at 20 °C. The suspensions were put into a folded capillary cell (model DTS1070, Malvern, UK) with a syringe to prevent the formation of air bubbles. Experiments were repeated ten times for each suspension, the average values and standard deviations were then calculated and reported in the appropriate figures.

Transmission Electron Microscopy

Transmission electron micrographs of microalgae ultrathin sections were taken with a JEOL JEM-1400 HC microscope equipped with a Gatan Orius SC1000B CCD camera. For the preparing of the ultrathin sections, the algae suspensions were first centrifuged at 280×g for 5 min. The supernatant was collected to prepare a 2.5% glutaraldehyde/2% paraformaldehyde solution that was used to fix the microalgae pellet at ambient temperature for 2 hours. The samples were then washed once with the supernatant and twice with water, before being chemically fixed with 1% osmium tetroxide for 1 hour, the excess fixative being removed by water washing. The microalgae pellet was then embedded in agarose (2%) and the consolidated sample, placed in an Eppendorf cone, was dehydrated in ascending ethanol series (25, 50, 70 and 90% for 15 min and three times in 100% for 30 min). The microalgae pellet in ethanol was then gradually infiltrated in epoxy resin (25, 50 and 75% for 1 h, and twice in 100% for 12 h) and polymerized in molds at 60 °C for 48 h. The ultrathin sections (80

nm thick), cut using an ultra-microtome fitted with a diamond knife (Leica UCT), were collected on Formvar-covered copper grids (Mesh 200) and stained with UranylAcetate to enhance contrast.

Theory

Soft Particle Theory

The Helmholtz–Smoluchowski equation (Equation (1)) is generally used to calculate from mobility measurements the potential at the shear plane surrounding the flowing particle, i.e., the zeta potential (ζ)³¹. The absolute values of the particle’s surface potential and the ζ potential differ theoretically, but in practice, they are often considered the same since they differ only slightly and the latter can be conveniently determined for hard particles from electrophoretic mobility measurements through:

$$\mu = \zeta \frac{\epsilon_0 \epsilon_r}{\eta} \quad (1)$$

where μ is the electrophoretic mobility, ϵ the vacuum permittivity, ϵ_r the dimensionless relative permittivity of the medium, and η the viscosity of the medium. This equation is valid only if the diffuse layer’s thickness is small compared to the particle size, i.e., $\kappa a \gg 1$, where κ is the Debye–Hückel parameter which is a function of the ionic strength and a is the particle radius. Furthermore, this equation was first developed to describe hard particles (non-deformable and non-permeable). Conversely, when the particle contains an outer shell permeable to electroosmotic flow (flow of electrolytes relative to a charged surface/particle due to an applied field³¹) and ions, i.e., in the case of a soft particle, the ζ potential cannot be strictly defined by Equation (1) anymore.

There is a fundamental difference in electrokinetic behavior between hard and soft particles: at high ionic strength, the electrophoretic mobility of a hard particle goes to zero

whereas that of a soft particle reaches a non-zero plateau³². Indeed, under high salt concentration conditions, the electric double layer is compressed, resulting in the screening of surface charges by solute ions, leading to zero mobility for hard particles. By contrast, the electrophoretic mobility of a soft particle originates from two phenomena: (i) the electric double layer, as for hard particles, and (ii) the electroosmotic flow within a permeable polyelectrolyte shell. The latter is responsible for a non-zero plateau value at high ionic strength^{16,32}.

The soft particle theory developed by Ohshima attempts to explain the electrokinetic behavior of soft colloidal particles. The main assumptions^{18,33} of this model are: (i) the Reynolds number of the liquid inside and outside the polymeric shell is small enough to neglect the inertial term of the Navier-Stokes equation; (ii) the applied electrical field is weak, thus, the particle velocity is proportional to the electrical field; (iii) the slipping plane is situated on the particle core surface; (iv) the particle core is impermeable to ions meanwhile the polyelectrolyte outer shell is permeable; (v) the charged groups are completely dissociated (no pH dependency) and uniformly distributed in the polyelectrolyte layer^{16,34}; (vi) the relative permittivity inside and outside the polymeric shell are equal.

In the case of biological cells, Ohshima and Kondo¹¹, through simplifications and new assumptions, reduced the initial complex set of equations describing the electrophoretic mobility to the following analytical expression:

$$\mu = \frac{\epsilon_0 \epsilon_r}{\eta} \frac{\psi_0 / \kappa_m + \psi_D / \lambda_{shell}}{1 / \kappa_m + 1 / \lambda_{shell}} + \frac{ZeN}{\eta \lambda_{shell}^2} \quad (2)$$

where ψ_D , and ψ_0 are the Donnan and surface potentials respectively (Figure 2), κ_m is the Debye-Hückel parameter of the polyelectrolyte layer, Z the valence of charged groups in the polymer shell, e the elementary charge, N the density of charged groups in the permeable polyelectrolyte shell and λ_{shell} the softness parameter of the polyelectrolyte layer. ψ_D , ψ_0 , and κ_m are given by Equations (3-5):

$$\psi_D = \frac{kT}{ze} \ln \left[\frac{ZN}{2zn^\infty} + \left\{ \left(\frac{ZN}{2zn^\infty} \right)^2 + 1 \right\}^{1/2} \right] \quad (3)$$

$$\psi_0 = \psi_D + \frac{2n^\infty kT}{ZeN} \left[1 - \left\{ \left(\frac{ZN}{2zn^\infty} \right)^2 + 1 \right\}^{1/2} \right] \quad (4)$$

$$\kappa_m = \kappa \left[1 + \left(\frac{ZN}{2zn^\infty} \right)^2 \right]^{1/4} \quad (5)$$

where k is the Boltzmann constant, T the temperature, z , and n^∞ are the valence, and the bulk concentration of the symmetrical electrolyte respectively. ψ_D , ψ_0 , and κ_m are functions of the ionic strength and consequently, the first term of Equation (2) tends to zero at high salt concentration, but the second term is constant. Therefore, this model can predict the non-zero plateau observed at high ionic strength as^{12,35}:

$$\mu_{plateau} \sim \frac{ZeN}{\eta \lambda_{shell}^2} \quad (6)$$

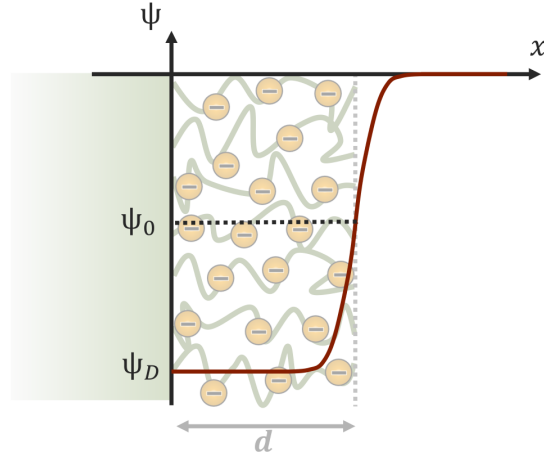


Figure 2: Schematic representation of the electric potential distribution of a soft particle. The particle is constituted of an impermeable non-charged core surrounded by a soft polyelectrolyte layer. In the present case, according to Equation (2), the polyelectrolyte layer d is thicker than the Debye length $1/\kappa$.

The quantity λ_{shell}^{-1} scales as a length and represents the characteristic penetration length of flow through the polymer shell³⁶. Equation (2) refers to the limiting case where: (i) particles are large with an uncharged core and homogeneous charge distribution within the polyelectrolyte layer; (ii) the hydrodynamic penetration length λ_{shell}^{-1} is significantly lower than the polymer shell's thickness d ($\lambda_{shell}d \gg 1$); (iii) the thickness d is much greater than the typical thickness of the electrical double layer κ^{-1} (Debye length); (iv) particles have low ZN and low electrical potentials in order to linearize the Poisson-Boltzmann equation (Debye-Hückel approximation)^{18,33}.

Moreover, Duval and Ohshima³⁶ highlighted that Equation (2) does not take into account the swelling properties of the polyelectrolyte and is limited to conditions in which polarization and relaxation of the electric double layer are absent. Despite these limitations, Equation (2) remains applicable for sufficiently high ionic strengths where polarization/relaxation effects are indeed negligible and the Debye-Hückel approximation is valid.

On the other hand, some studies applied numerical solutions with fewer assumptions to successfully fit the experimental data at several ionic strengths^{29,36,37}. For instance, Pagnout et al.³⁷ studied the electrophoresis of *Escherichia coli* bacteria with different surface structures. The authors correlated the electrokinetic measurements with analytical and rigorous numerical resolutions of the electrohydrodynamics of soft diffuse particles, i.e., taking into account the swelling process of the polyelectrolyte layer and the non-linear Poisson-Boltzmann equation with full integration of double layer polarization/relaxation³⁶.

Electrostatic Interaction

In order to evaluate the colloidal stability of microalgae suspensions in light of soft particle theory, we must analyze the electrostatic forces at play. Ohshima³⁸ derived an expression of electrostatic energy between two spherical particles with the help of Derjaguin's approximation, which can be applied to both hard and soft particles. This expression is given by:

$$V(H) = \frac{4\pi a_1 a_2}{a_1 + a_2} \epsilon_0 \epsilon_r \psi_{\text{eff1}} \psi_{\text{eff2}} e^{-\kappa H} \quad (7)$$

where H is the distance between the two particles, a_1 and a_2 are the radius of spheres 1 and 2, and ψ_{eff1} and ψ_{eff2} are the effective surface potentials of spheres 1 and 2. Equation (7) is obtained using a linear superposition approximation (LSA) method.

According to Equation (7), the electrostatic energy is proportional to the particle's surface potential. If the charges of the particles are of the same sign, the electrostatic interaction is repulsive. Therefore, by comparing the effective ζ potential (Equation (1)) to the surface potential obtained using the soft particle theory (Equation (4)), it is possible to evaluate the difference between the predicted electrostatic repulsion using the approach of hard or soft particles.

In summary, Equation (7) represents a limiting case for soft particles where: (i) ψ_D represents the potential deep inside the polyelectrolyte layer, i.e., $\lambda_{\text{shell}}^{-1}$ is much smaller than the thickness of the polymer shell d ($\lambda_{\text{shell}} d \gg 1$); (ii) The Debye-Hückel's approximation is valid, i.e., low charged interface and low potential conditions; (iii) Derjaguin's integration is applicable, i.e., the particle size is much greater than the Debye Length, κ^{-1} ; (iv) LSA is valid, i.e., the particles are far apart ($\kappa H \gg 1$); (v) The particles are assumed to be surrounded by an homogeneous shell^{39,40}. This equation represents an analytical solution of the electrostatic forces between soft particles, Duval et al.³⁹ developed numerical resolutions with fewer assumptions.

Results and Discussion

Electrokinetic Behavior

The electrophoretic mobility of the three different microalgae species was measured as a function of ionic strength (KNO_3) and the results are reported in Figure 3. All three microalgae show negative values of electrophoretic mobility, reflecting, as expected, the overall negative surface charge of those microorganisms. In all cases, when salt concentration increases, the mobility becomes less negative due to the screening of the diffusive double layer. However, the mobility does not go to zero, even at high ionic strength. On the contrary, the mobility tends to a non-zero plateau (better observed in linear scale, Figure S1), a behavior typical of soft particles (Equation (6))³³. These results thus suggest that these microorganisms carry a charged and permeable polyelectrolyte type layer. According to Equation (2),

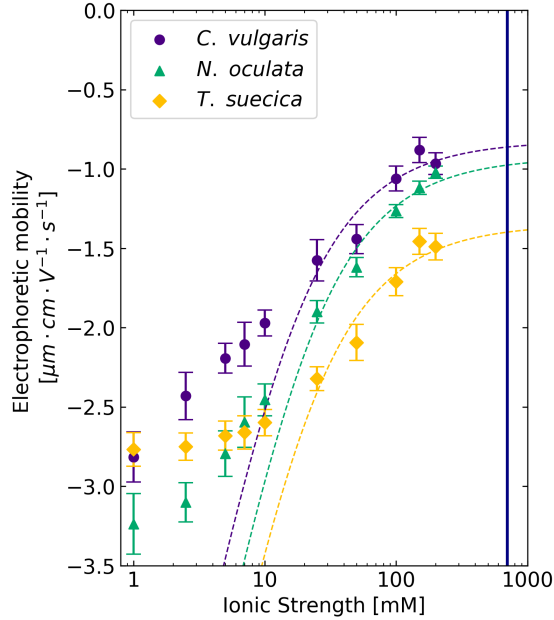


Figure 3: Electrophoretic mobility as a function of solution ionic strength (KNO_3) for three microalgae species: *C. vulgaris*, *N. oculata*, and *T. suecica*. The markers represent the average experimental mobility measurements, error bars correspond to standard deviations and the dashed line is a fit of experimental data at a high salt concentration to Equation (2). The vertical blue line corresponds approximately to the ionic strength of seawater.

the residual finite mobility should only depend on the fixed charged density and the flow permeability of the outer shell.

A typical value for the ionic strength of sea water (see for example ASTM standard D1141-98(2013) artificial seawater⁴¹) is approximately 700 mM (vertical blue line in Figure 3). However, due to the degradation of the electrodes from the capillary cell at higher ionic strengths, mobility measurements were made only on samples with ionic strength below 200 mM. Since a plateau was found from approximately 150 mM, it can be expected that the electrophoretic mobility at sea water ionic strengths is equal to the plateau value for each microalgae species.

To obey the criteria of $\kappa d \gg 1$ assumed in the derivation of Equation (2), the quantitative analysis was restricted to salt concentrations greater than 10 mM. Nonlinear least-squares minimization using the Levenberg-Marquardt algorithm implemented by LMFIT Python package⁴² was used to fit the experimental data to Equation (2) (dashed lines in Figure 3). The quantities ZN and λ_{shell}^{-1} obtained for each microalga from the best fit are listed in Table 1, these results are comparable with the values for others microorganisms^{16,21}. At low salt concentrations, the mobility of microalgae does not fit the model well, as can be seen in Figure 3. Many studies observed similar deviation in other soft particles at low ionic strength. This observation was attributed to polarization/relaxation of the electric double layer that is neglected in Equation (2), to the non-homogeneous fixed charges distribution within the polyelectrolyte layer and to the high electric potentials experimented at low ionic

Table 1: Values of charge density ZN (in mM) and hydrodynamic penetration length λ_{shell}^{-1} (in nm) for *C.vulgaris*, *N. oculata*, and *T. suecica* obtained from fitting of experimental data at high salt concentration (> 10 mM) to Equation (2).

Microalgae	ZN [mM]	λ_{shell}^{-1} [nm]
<i>C. vulgaris</i>	-33	1.6
<i>N. oculata</i>	-43	1.5
<i>T. suecica</i>	-42	1.8

strength (i.e., Debye-Hückel’s approximation is not valid)^{29,30,33,43}.

All the characteristic hydrodynamic penetration length values in the outer shell (λ_{shell}^{-1}) found by fitting experimental data to Equation (2) ranged from one to two nanometers for the three microalgae species studied (Table 1). Concerning the permeable layer charge concentration, *N. oculata* and *T. suecica* exhibit a higher charge concentration than *C. vulgaris* (Table 1). Moreover, *N. oculata* and *C. vulgaris* have a slightly lower penetration length (λ_{shell}^{-1}) reflecting a possibly less permeable surface than *T. suecica*.

Confidence Interval

In order to investigate the significance of values obtained from the best fit, the confidence interval of parameters ZN and λ_{shell} were estimated using the LMFIT Python package. Results are shown in Table S1 in the Supplementary Information. LMFIT uses the F-test to obtain these confidence intervals. It compares the null model (the best fit found) with an alternative model, where one of the parameters is fixed to a specific value⁴².

Table S1 shows the best-fit values for the parameters, and parameter values that are at the varying confidence levels given by steps in σ (standard deviation), from 1- σ (68.27% confidence) to 3- σ (99.73% confidence). The errors are asymmetric; this is due to the complexity of the model used which comes from Equation (2).

Plots of the confidence region are shown in Figure 4; they have an elongated and curved shape. The surfaces reveal a small darker area corresponding to a high confidence level. From Table S1 and Figure 4, it can be observed that the fit is in general more sensitive to variations of λ_{shell}^{-1} than to variations in ZN .

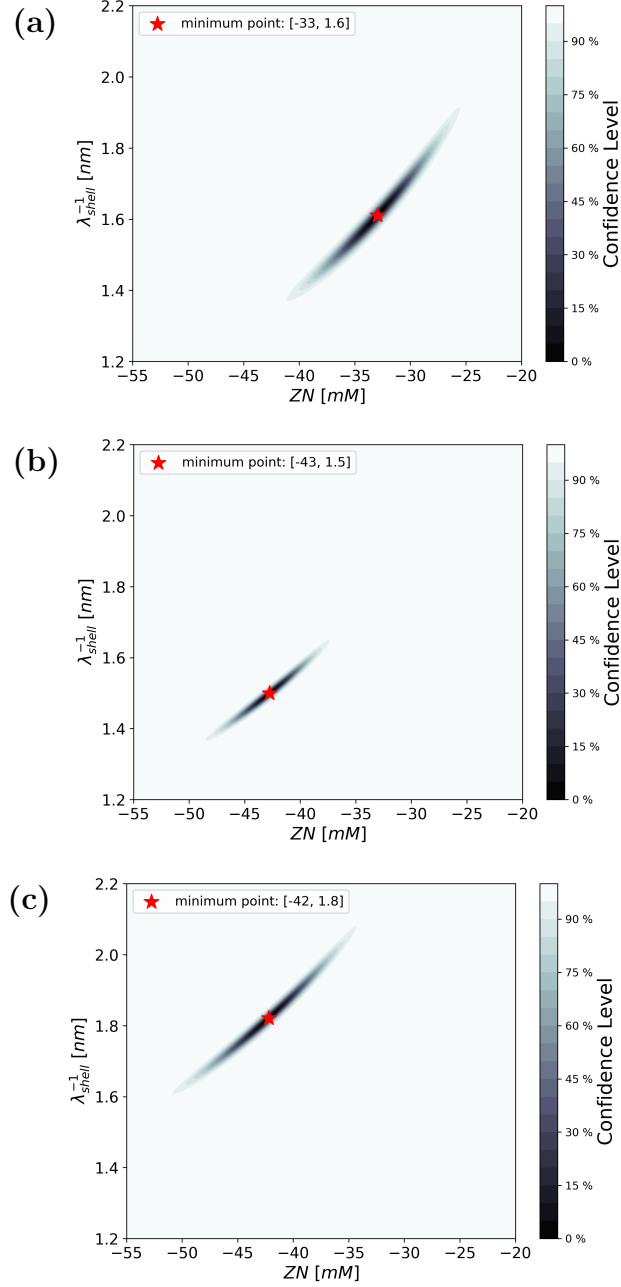


Figure 4: Confidence intervals obtained using LMFIT Python package for the charge density of the polymeric layer, ZN , and the hydrodynamic penetration length, λ_{shell}^{-1} , for three microalgae species **(a)** *C. vulgaris*, **(b)** *N. oculata*, and **(c)** *T. suecica*.

Surface Potential

As mentioned in the introduction, the use of zeta potential to quantify the charge of microalgae is physically inappropriate. Indeed, using Equation (4), it is possible to estimate

the outer surface potential of microalgae at different ionic strengths. Figure 5 compares these values to the apparent zeta potential calculated from the Helmholtz–Smoluchowski Equation (1). It can be observed that the surface potentials of *N. oculata* and *T. suecica* have approximately the same value at all probed ionic strength. This is because the surface potential calculated from Equation (4) only depends on the ionic strength and the polyelectrolyte layer’s charge density ZN , and this latter value is similar for these two microalgae (Table 1). At high ionic strength, ψ_0 tends to zero for all three algal strains: this behavior can be attributed to the suppression of the surface potential due to the compression of the electric double layer³³. By contrast, the non-zero electrophoretic mobility at high ionic strength imposes to consider non-zero apparent ζ potential, an unrealistic occurrence under such conditions where the Debye length tends to zero.

As seen in Figure 5, the absolute values of the outer surface potential (ψ_0) of microalgae,

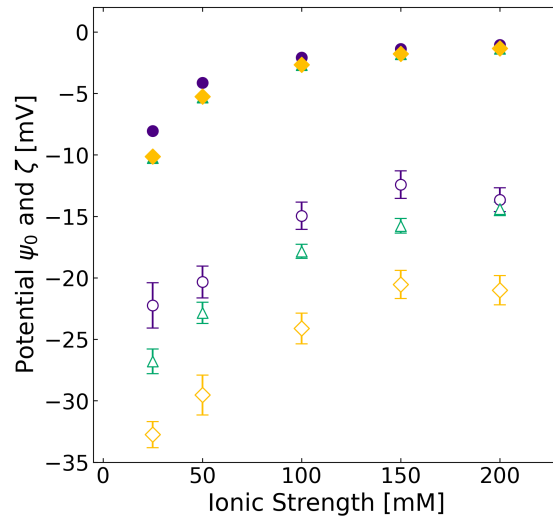


Figure 5: Surface potential (filled markers), ψ_0 , and zeta potential, ζ (open markers) as a function of ionic strength of three microalgae species: *C. vulgaris* (●), *N. oculata* (▲), and *T. suecica* (◆). The outer surface potentials, ψ_0 , were determined from the fitting of the measured electrophoretic mobilities to Ohshima’s theory (Equation (2)). The apparent zeta potentials, ζ , were calculated from the measured electrophoretic mobilities using the Helmholtz–Smoluchowski Equation (1). Error bars correspond to standard deviations.

obtained applying Ohshima’s formalism, are smaller than the absolute value of the ζ potential, obtained following the Helmholtz–Smoluchowski equation. This indicates that the electrostatic force is smaller using ψ_0 as the effective surface potential in Equation (7) than using ζ ^{44,45}. In other words, the expected electrostatic repulsion between cells is notably smaller than that usually expected when simply considering ζ potentials that do not take into account the soft character of microalgae^{10,46}. In other words, the electrostatic contribution to the colloidal stability of microalgae cells in suspension might be less important than expected from ζ potentials measurements.

Microalgae Morphology

In complement to the electrophoretic mobility measurements, the surface morphology of microalgae was investigated under optical and TEM microscopy. The results are shown in Figure 6. *Chlorella vulgaris* has a spherical to ellipsoidal shape, with a mean diameter of 4 μm in the growth phase (Figure 6a). Its cell wall is composed of electron-dense layers with short fibers which protrude from the outer layer (Figures 6d and 6g). The microalgae’s cell wall varies according to the cell growth stage and environmental conditions⁴⁷. By measuring the thickness of the new daughter cell wall at different growth phases, Yamamoto et al.⁴⁸ classified *C. vulgaris* as an early type species, meaning that synthesis of the daughter cell wall begins at the early growth phase. This implies that the cell wall of *C. vulgaris* is thinner initially and gets thicker at the beginning of the growth phase due the formation of a daughter cell wall between the mother cell wall and the plasma membrane⁴⁹. The cell wall thickness of *C. vulgaris* cells observed by TEM (Figure 6g) is between 50 and 150 nm, which may correspond to a combination of mother and daughter cell walls. Most interestingly, a layer of EPS extending away from the surface is apparent with a thickness in the range of 10 nm.

Nannochloropsis oculata is a small green spherical or oval cell measuring around 2 μm in diameter (Figures 6b and 6e). As shown by TEM (Figure 6h), the *N. oculata* cell wall is

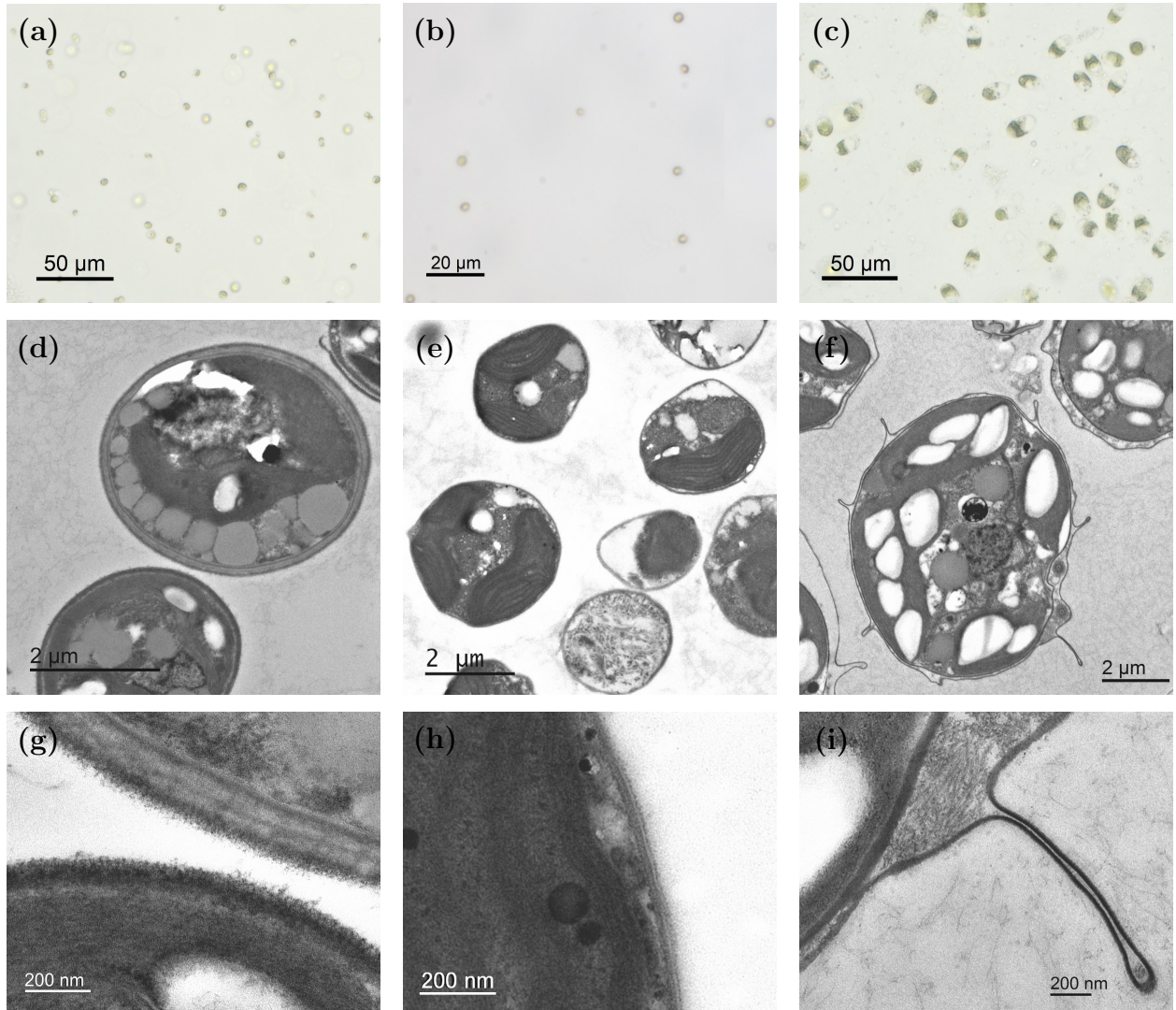


Figure 6: Light microscopic micrographs at 20X magnification of (a) *C. vulgaris*, (b) *N. oculata* and (c) *T. suecica* suspensions after sample preparation for electrophoretic mobility measurements at 1 mM KNO₃. Transmission electron micrographs of (d)-(g) *C. vulgaris*, (e)-(h) *N. oculata* and (f)-(i) *T. suecica*.

composed of two layers and extensions protruding from the outer surface, with a cell wall thickness varying from 30-100 nm. The bilayer of the genus *Nannochloropsis* is composed of an inner cellulose layer and an outer algaenan layer⁵⁰. A layer of EPS is also observed, albeit less evident than in the *Chlorella vulgaris* case.

Tetraselmis suecica has an elongated shape and is 10-20 μm in length. It is a flagellated species, however, it was verified by optical microscopy that these cells lost their flagella during the centrifugation step of the samples preparation for electrophoretic mobility measurements (Figure 6c). From TEM micrographs (Figures 6f and 6i), it is possible to observe a three-layer outer structure composed of a median electron-translucent layer between two electron-dense layers with fibers extending from outer layer. This structure can be attributed to the mother (outer layer) and daughter (inner layer) cell walls of *T. suecica*. When the mother cell wall breaks, the release of daughter cells occurs⁵¹. Daughter and mother cell wall thicknesses vary from 20-90 nm. Once again, a layer of EPS extend from the cells surfaces.

For all three species investigated, fiber structures were identified in the outermost surface layer corresponding to EPS layer. This EPS layer thicknesses observed on the TEM images (Figures 6g to 6i) were in few tens of nanometers and can be identified with the permeable shell evidenced from electrokinetics considerations. This results along with the estimated hydrodynamic penetration lengths (λ_{shell}^{-1} in Table 1) are in accordance with Equation (2) assumption that $\lambda_{shell}d \gg 1$.

TEM has potential artifacts from sample preparation, therefore the dimensions obtained from TEM micrographs are not necessarily exact, but they remain representative of what occurs in suspension and of the actual state of the microalgae cells under investigation.

Conclusion

In the present work, we studied the electrostatic behavior of three microalgae species: *C. vulgaris*, *N. oculata*, and *T. suecica* in solution as a function of the ionic strength using electrophoretic experiments. The variation of electrophoretic mobility with ionic strength was adjusted to the soft particle theory, confirming the soft nature of these microorganisms characterized by having an outer permeable layer. It transpired that the ζ potential is not a pertinent parameter to describe algal cell electrokinetic behavior and cannot be used to


assess surface charge potential. An important consequence is that electrostatic phenomena might contribute less than usually expected to the colloidal stability of microalgae and that the balance between repulsive electrostatic and attractive hydrophobic interactions^{52,53} should be reconsidered using the soft particle theory. The role of the charges within the extracellular polymeric substances' corona around the microalgae cell walls is then essential in controlling their flocculation and adhesion,^{54,55} but cannot be comprehended solely through the measurement of an effective ζ potential. This study is thus a starting point for a better understanding of the colloidal behavior of microalgae in their natural environment or for devising new ways to improve microalgae harvesting, reducing overall energy consumption during microalgae production.

Supporting Information Available


Electrophoretic mobility as a function of ionic strength in linear scale (Figure SI-1) and confidence intervals obtained by LMFIT (Table SI-1).

Author Information


Corresponding Authors


Jean-Baptiste d'Espinose de Lacaillerie – Soft Matter Sciences and Engineering Laboratory, ESPCI Paris, Université PSL, Sorbonne Université, CNRS UMR 7615, 10 Rue Vauquelin, F-75005 Paris, France; Laboratoire Physico-Chimie des Interfaces Complexes, ESPCI Paris, 10 Rue Vauquelin, F-75231 Paris, France;  orcid.org/0000-0002-2463-6877; E-mail: jean-baptiste.despinose@espci.fr


Nicolas Sanson – Soft Matter Sciences and Engineering Laboratory, ESPCI Paris, Université PSL, Sorbonne Université, CNRS UMR 7615, 10 Rue Vauquelin, F-75005 Paris, France; Laboratoire Physico-Chimie des Interfaces Complexes, ESPCI Paris, 10 Rue Vauquelin,


F-75231 Paris, France;  orcid.org/0000-0002-7678-0440; E-mail: nicolas.sanson@espci.fr


Authors

Paula Araujo Gomes – Soft Matter Sciences and Engineering Laboratory, ESPCI Paris, Université PSL, Sorbonne Université, CNRS UMR 7615, 10 Rue Vauquelin, F-75005 Paris, France; Laboratoire Physico-Chimie des Interfaces Complexes, ESPCI Paris, 10 Rue Vauquelin, F-75231 Paris, France; TotalEnergies OneTech, Pôle d’Etudes et Recherche de Lacq, BP 47, 64170 Lacq, France;  orcid.org/0000-0002-9300-0442

Bruno Lartiges – Géosciences Environnement Toulouse (GET), Université de Toulouse 3 (Paul Sabatier), 14 Avenue Edouard Belin, 31400 Toulouse, France;  orcid.org/0000-0003-1387-9942

Martin Maliet – Soft Matter Sciences and Engineering Laboratory, ESPCI Paris, Université PSL, Sorbonne Université, CNRS UMR 7615, 10 Rue Vauquelin, F-75005 Paris, France;  orcid.org/0000-0003-0653-4786

Valérie Molinier – TotalEnergies OneTech, Pôle d’Etudes et Recherche de Lacq, BP 47, 64170 Lacq, France; Laboratoire Physico-Chimie des Interfaces Complexes, Bâtiment CHEMSTARTUP, Route Départemental 817, 64170 Lacq, France;  orcid.org/0000-0001-5035-7620

Nicolas Passade-Boupat – TotalEnergies OneTech, Pôle d’Etudes et Recherche de Lacq, BP 47, 64170 Lacq, France; Laboratoire Physico-Chimie des Interfaces Complexes, Bâtiment CHEMSTARTUP, Route Départemental 817, 64170 Lacq, France;  orcid.org/0000-0003-2913-0864

Author Contributions

Paula Araujo Gomes – Main investigator. Algal culture and all experiments except TEM. Conceptualization, Methodology, Investigation, Formal analysis, Visualization, Writing – Original Draft; **Jean-Baptiste d’Espinose de Lacaillerie** – Conceptualization,

Methodology, Project administration, Supervision, Writing – Review and Editing. **Bruno Lartiges** – TEM experiments; Conceptualization, Methodology, Writing – Review and Editing; **Martin Maliet** – Algal culture and electrophoretic measurements; **Valérie Molinier** – Supervision, Project administration, Writing – Review and Editing; **Nicolas Passade-Boupat** – Project administration, Writing – Review and Editing; **Nicolas Sanson** – Conceptualization, Methodology, Project administration, Supervision, Writing – Review and Editing.

Notes

The authors declare no competing financial interest.

Acknowledgement

BL thanks Vanessa Soldan (METI) for precious help with resin embedding of microalgae. The authors are thankful to Jérôme F. L. Duval (LIEC, Nancy, France) for helpful discussion about soft particle theory.

Funding Sources

This study was supported by TotalEnergies OneTech (Lacq, France). PAG’s doctoral thesis is funded by TotalEnergies OneTech through a CIFRE ANRT fellowship N° 2021/0655.

References

- (1) Luiten, E. E. M.; Akkerman, I.; Koulman, A.; Kamermans, P.; Reith, H.; Barbosa, M. J.; Sipkema, D.; Wijffels, R. H. Realizing the promises of marine biotechnology. *Biomol. Eng.* **2003**, *20*, 429–439.

- (2) Garrido-Cardenas, J. A.; Manzano-Agugliaro, F.; Acien-Fernandez, F. G.; Molina-Grima, E. Microalgae research worldwide. *Algal Res.* **2018**, *35*, 50–60.
- (3) Lam, M. K.; Lee, K. T.; Mohamed, A. R. Current status and challenges on microalgae-based carbon capture. *Int. J. Greenhouse Gas Control* **2012**, *10*, 456–469.
- (4) Vandamme, D.; Foubert, I.; Muylaert, K. Flocculation as a low-cost method for harvesting microalgae for bulk biomass production. *Trends Biotechnol.* **2013**, *31*, 233–239.
- (5) Kumar, N.; Banerjee, C.; Negi, S.; Shukla, P. Microalgae harvesting techniques: updates and recent technological interventions. *Crit. Rev. Biotechnol.* **2022**, *0*, 1–27.
- (6) Najjar, Y. S.; Abu-Shamleh, A. Harvesting of microalgae by centrifugation for biodiesel production: A review. *Algal Res.* **2020**, *51*, 102046.
- (7) Branyikova, I.; Prochazkova, G.; Potocar, T.; Jezkova, Z.; Branyik, T. Harvesting of microalgae by flocculation. *Fermentation* **2018**, *4*, 93.
- (8) Xiao, R.; Zheng, Y. Overview of microalgal extracellular polymeric substances (EPS) and their applications. *Biotechnol. Adv.* **2016**, *34*, 1225–1244.
- (9) Zeng, W.; Li, P.; Huang, Y.; Xia, A.; Zhu, X.; Zhu, X.; Liao, Q. How Interfacial Properties Affect Adhesion: An Analysis from the Interactions between Microalgal Cells and Solid Substrates. *Langmuir* **2022**, *38*, 3284–3296.
- (10) Zhang, X.; Yuan, H.; Wang, Y.; Guan, L.; Zeng, Z.; Jiang, Z.; Zhang, X. Cell Surface Energy Affects the Structure of Microalgal Biofilm. *Langmuir* **2020**, *36*, 3057–3063.
- (11) Ohshima, H.; Kondo, T. On the electrophoretic mobility of biological cells. *Biophys. Chem.* **1991**, *39*, 191–198.
- (12) Ohshima, H. Electrophoresis of soft particles. *Adv. Colloid Interface Sci.* **1995**, *62*, 189–235.

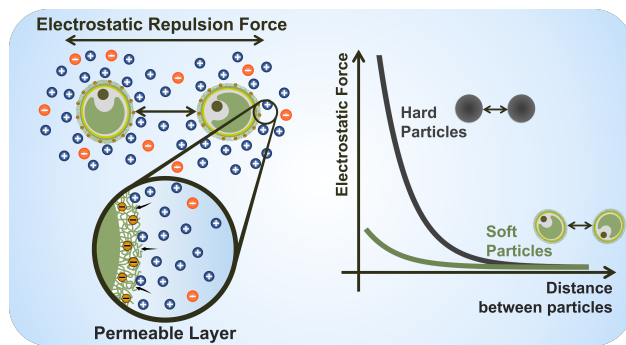
- (13) Saville, D. Electrokinetic Properties of Fuzzy Colloidal Particles. *J. Colloid Interface Sci.* **2000**, *222*, 137–145.
- (14) Hill, R. J.; Saville, D.; Russel, W. Electrophoresis of spherical polymer-coated colloidal particles. *J. Colloid Interface Sci.* **2003**, *258*, 56–74.
- (15) López-García, J.; Grosse, C.; Horno, J. Numerical study of colloidal suspensions of soft spherical particles using the network method: 1. DC electrophoretic mobility. *J. Colloid Interface Sci.* **2003**, *265*, 327–340.
- (16) Duval, J. F. L.; Gaboriaud, F. Progress in electrohydrodynamics of soft microbial particle interphases. *Curr. Opin. Colloid Interface Sci.* **2010**, *15*, 184–195.
- (17) Ashrafizadeh, S. N.; Seifollahi, Z.; Ganjizade, A.; Sadeghi, A. Electrophoresis of spherical soft particles in electrolyte solutions: A review. *Electrophoresis* **2020**, *41*, 81–103.
- (18) Ohshima, H. Electrophoresis of soft particles: Analytic approximations. *Electrophoresis* **2006**, *27*, 526–533.
- (19) Maurya, S. K.; Gopmandal, P. P.; Ohshima, H.; Duval, J. F. L. Electrophoresis of composite soft particles with differentiated core and shell permeabilities to ions and fluid flow. *J. Colloid Interface Sci.* **2020**, *558*, 280–290.
- (20) Ohshima, H. Approximate analytic expressions for the electrophoretic mobility of spherical soft particles. *Electrophoresis* **2021**, *42*, 2182–2188.
- (21) Louie, S. M.; Phenrat, T.; Small, M. J.; Tilton, R. D.; Lowry, G. V. Parameter Identifiability in Application of Soft Particle Electrokinetic Theory To Determine Polymer and Polyelectrolyte Coating Thicknesses on Colloids. *Langmuir* **2012**, *28*, 10334–10347.
- (22) Fernández-Nieves, A.; Márquez, M. Electrophoresis of ionic microgel particles: From charged hard spheres to polyelectrolyte-like behavior. *J. Chem. Phys.* **2005**, *122*, 084702.

- (23) Daly, E.; Saunders, B. R. Temperature-dependent electrophoretic mobility and hydrodynamic radius measurements of poly (*N*-isopropylacrylamide) microgel particles: structural insights. *Phys. Chem. Chem. Phys.* **2000**, *2*, 3187–3193.
- (24) Duval, J. F. L.; Wilkinson, K. J.; van Leeuwen, H. P.; Buffle, J. Humic Substances Are Soft and Permeable: Evidence from Their Electrophoretic Mobilities. *Environ. Sci. Technol.* **2005**, *39*, 6435–6445.
- (25) Makino, K.; Yamamoto, S.; Fujimoto, K.; Kawaguchi, H.; Ohshima, H. Surface Structure of Latex Particles Covered with Temperature-Sensitive Hydrogel Layers. *J. Colloid Interface Sci.* **1994**, *166*, 251–258.
- (26) Ho, C.; Kondo, T.; Muramatsu, N.; Ohshima, H. Surface Structure of Natural Rubber Latex Particles from Electrophoretic Mobility Data. *J. Colloid Interface Sci.* **1996**, *178*, 442–445.
- (27) Karreman, R. J.; Dague, E.; Gaboriaud, F.; Quilès, F.; Duval, J. F. L.; Lindsey, G. G. The stress response protein Hsp12p increases the flexibility of the yeast *Saccharomyces cerevisiae* cell wall. *Biochim. Biophys. Acta, Proteins Proteomics* **2007**, *1774*, 131–137.
- (28) Shamrock, V. J.; Duval, J. F. L.; Lindsey, G. G.; Gaboriaud, F. The role of the heat shock protein Hsp12p in the dynamic response of *Saccharomyces cerevisiae* to the addition of Congo red. *FEMS Yeast Res.* **2009**, *9*, 391–399.
- (29) Gaboriaud, F.; Gee, M. L.; Strugnell, R.; Duval, J. F. L. Coupled Electrostatic, Hydrodynamic, and Mechanical Properties of Bacterial Interfaces in Aqueous Media. *Langmuir* **2008**, *24*, 10988–10995.
- (30) Sonohara, R.; Muramatsu, N.; Ohshima, H.; Kondo, T. Difference in surface properties between *Escherichia coli* and *Staphylococcus aureus* as revealed by electrophoretic mobility measurements. *Biophys. Chem.* **1995**, *55*, 273–277.

- (31) Masliyah, J. H.; Bhattacharjee, S. *Electrokinetic and colloid transport phenomena*; John Wiley & Sons, 2006; pp 295–361.
- (32) Dukhin, S. S.; Zimmermann, R.; Werner, C. Electrophoresis of soft particles at high electrolyte concentrations: An interpretation by the Henry theory. *J. Colloid Interface Sci.* **2007**, *313*, 676–9.
- (33) de Kerchove, A. J.; Elimelech, M. Relevance of electrokinetic theory for “soft” particles to bacterial cells: implications for bacterial adhesion. *Langmuir* **2005**, *21*, 6462–6472.
- (34) Duval, J. F. L.; Busscher, H. J.; van de Belt-Gritter, B.; van der Mei, H. C.; Norde, W. Analysis of the Interfacial Properties of Fibrillated and Nonfibrillated Oral *Streptococcal* Strains from Electrophoretic Mobility and Titration Measurements: Evidence for the Shortcomings of the ‘Classical Soft-Particle Approach’. *Langmuir* **2005**, *21*, 11268–11282.
- (35) Makino, K.; Ohshima, H. Soft particle analysis of electrokinetics of biological cells and their model systems. *Sci. Technol. Adv. Mater.* **2011**, *12*, 023001.
- (36) Duval, J. F. L.; Ohshima, H. Electrophoresis of Diffuse Soft Particles. *Langmuir* **2006**, *22*, 3533–3546.
- (37) Pagnout, C.; Présent, R. M.; Billard, P.; Rotureau, E.; Duval, J. F. L. What do luminescent bacterial metal-sensors probe? Insights from confrontation between experiments and flux-based theory. *Sens. Actuators, B* **2018**, *270*, 482–491.
- (38) Ohshima, H. *Electrical Phenomena at Interfaces and Biointerfaces: Fundamentals and Applications in Nano-, Bio-, and Environmental Sciences*; John Wiley & Sons, 2012; Chapter 2, pp 17–26.
- (39) Duval, J. F. L.; Merlin, J.; Narayana, P. A. L. Electrostatic interactions between diffuse

- soft multi-layered (bio) particles: beyond Debye–Hückel approximation and Deryagin formulation. *Phys. Chem. Chem. Phys.* **2011**, *13*, 1037–1053.
- (40) Ohshima, H. Electrostatic interaction of soft particles. *Adv. Colloid Interface Sci.* **2015**, *226*, 2–16.
- (41) ASTM D1141-98, *Standard Practice for the Preparation of Substitute Ocean Water*; Standard, (Reapproved 2003); Vol. 2000.
- (42) Newville, M.; Stensitzki, T.; Allen, D. B.; Rawlik, M.; Ingargiola, A.; Nelson, A. LM-FIT: Non-linear least-square minimization and curve-fitting for Python. *Astrophysics Source Code Library* **2016**, ascl-1606.
- (43) Vouriot, E.; Bihannic, I.; Beaussart, A.; Waldvogel, Y.; Razafitianamaharavo, A.; Ribeiro, T.; Farinha, J. P. S.; Beloin, C.; Duval, J. F. L. Electrophoresis as a simple method to detect deleterious actions of engineered nanoparticles on living cells. *Environ. Chem.* **2019**, *17*, 39–53.
- (44) Morisaki, H.; Nagai, S.; Ohshima, H.; Ikemoto, E.; Kogure, K. The effect of motility and cell-surface polymers on bacterial attachment. *Microbiology* **1999**, *145*, 2797–2802.
- (45) Hori, K.; Matsumoto, S. Bacterial adhesion: From mechanism to control. *Biochem. Eng. J.* **2010**, *48*, 424–434.
- (46) Ozkan, A.; Berberoglu, H. Physico-chemical surface properties of microalgae. *Colloids Surf., B* **2013**, *112*, 287–293.
- (47) Safi, C.; Zebib, B.; Merah, O.; Pontalier, P.-Y.; Vaca-Garcia, C. Morphology, composition, production, processing and applications of *Chlorella vulgaris*: A review. *Renewable Sustainable Energy Rev.* **2014**, *35*, 265–278.
- (48) Yamamoto, M.; Kurihara, I.; Kawano, S. Late type of daughter cell wall synthesis in

- one of the *Chlorellaceae*, *Parachlorella kessleri* (*Chlorophyta*, *Trebouxiophyceae*). *Planta* **2005**, *221*, 766–775.
- (49) Baudalet, P.-H.; Ricochon, G.; Linder, M.; Muniglia, L. A new insight into cell walls of *Chlorophyta*. *Algal Res.* **2017**, *25*, 333–371.
- (50) Scholz, M. J.; Weiss, T. L.; Jinkerson, R. E.; Jing, J.; Roth, R.; Goodenough, U.; Posewitz, M. C.; Gerken, H. G. Ultrastructure and composition of the *Nannochloropsis gaditana* cell wall. *Eukaryotic Cell* **2014**, *13*, 1450–1464.
- (51) Abiusi, F.; Sampietro, G.; Marturano, G.; Biondi, N.; Rodolfi, L.; D'Ottavio, M.; Tredici, M. R. Growth, photosynthetic efficiency, and biochemical composition of *Tetraselmis suecica* F&M-M33 grown with LEDs of different colors. *Biotechnol. Bioeng.* **2014**, *111*, 956–964.
- (52) Yuan, H.; Zhang, X.; Jiang, Z.; Chen, X.; Zhang, X. Quantitative Criterion to Predict Cell Adhesion by Identifying Dominant Interaction between Microorganisms and Abiotic Surfaces. *Langmuir* **2019**, *35*, 3524–3533.
- (53) Zeng, W.; Huang, Y.; Xia, A.; Liao, Q.; Chen, K.; Zhu, X.; Zhu, X. Thermoresponsive Surfaces Grafted by Shrinkable Hydrogel Poly(*N* -isopropylacrylamide) for Controlling Microalgae Cells Adhesion during Biofilm Cultivation. *Environ. Sci. Technol.* **2021**, *55*, 1178–1189.
- (54) Chen, Z.; Qiu, S.; Yu, Z.; Li, M.; Ge, S. Enhanced Secretions of Algal Cell-Adhesion Molecules and Metal Ion-Binding Exoproteins Promote Self-Flocculation of *Chlorella* sp. Cultivated in Municipal Wastewater. *Environ. Sci. Technol.* **2021**, *55*, 11916–11924.
- (55) Demir, I.; Blockx, J.; Dague, E.; Guiraud, P.; Thielemans, W.; Muylaert, K.; Formosa-Dague, C. Nanoscale Evidence Unravels Microalgae Flocculation Mechanism Induced by Chitosan. *ACS Appl. Bio Mater.* **2020**, *3*, 8446–8459.



For Table of Contents Only